# Longshore Transport Variability of Beach Face Grain Size: Implications for Dune Evolution

Authors: Hallin, Caroline, Almström, Björn, Larson, Magnus, and Hanson, Hans

Source: Journal of Coastal Research, 35(4) : 751-764

Published By: Coastal Education and Research Foundation

URL: https://doi.org/10.2112/JCOASTRES-D-18-00153.1

| Journal of Coastal Research | 35 | 4 | 751–764 | Coconut Creek, Florida | July 2019 |
|---|---|---|---|---|---|

# Longshore Transport Variability of Beach Face Grain Size: Implications for Dune Evolution

**Caroline Hallin*, Björn Almström, Magnus Larson, and Hans Hanson**

Department of Water Resources Engineering
Lund University
Lund 221 00, Sweden

www.cerf-jcr.org

www.JCRonline.org

**ABSTRACT**

Hallin, C.; Almström, B.; Larson, M., and Hanson, H., 2019. Longshore transport variability of beach face grain size: Implications for dune evolution. *Journal of Coastal Research,* 35(4), 751–764. Coconut Creek (Florida), ISSN 0749-0208.

This study investigates grain-size sorting through longshore transport processes and how it influences dune evolution. The analysis is based on a data set of 58 sediment samples distributed alongshore over a 6.5-km-long sandy beach in Ängelholm, Sweden. Grain size differs significantly from north to south, where median grain size varies from about 0.4–0.15 mm. The long-term coastal evolution is derived from shoreline change analysis of a series of aerial photos from the 1940s until today and from longshore sediment transport rates calculated on the basis of wave data simulated by the SWAN wave model employed in the Coastal Engineering Research Center (CERC) formula. The results show an almost unidirectional longshore transport from north to south; the beach is eroding in the northern part and accreting in the southern part. The McLaren model, a grain size–based model to predict transport direction, was tested against the grain size data. The test indicated transport in the opposite direction. This result supports previous studies suggesting that the McLaren model has limited applicability for sandy beaches with a dominant longshore transport. The sediment samples were collected at the mid–beach face position in an area where sediment is supplied to the beach during accreting conditions. Sediment in the appropriate grain size to build dunes—at this beach, 0.2–0.3 mm—was found in the parts of the beach where the dunes are growing. In the eroding parts, the sediment was coarser, suggesting that the longshore transport influences the supply of sediment for aeolian transport. The gradients in longshore transport rate were also found to affect dune morphology; the dunes were higher in the eroding and stable parts of the beach and lower in the accreting parts.

**ADDITIONAL INDEX WORDS:** *Median grain size, McLaren model, grain-size sorting, reference grain size.*

## INTRODUCTION

Because transport processes sort sediment through selection by weight, grain size, and form during pick-up and deposition, sediment transport patterns are reflected in the spatial distribution of grain sizes (Ramsey and Galvin, 1977; Trask and Hand, 1985). In sandy systems, finer particles are more easily entrained, typically leading to coarsening of sediment in eroding areas and accumulation of finer sediments where the sand is deposited (Self, 1977). This variation of supply and sediment sorting by transport processes affects the dune morphology (Ollerhead *et al.*, 2013; Psuty, 1988; Sherman and Bauer, 1993). On accreting beaches, the dunes are typically lower, because they do not have time to grow in height before a new foredune is built in front of them (Hesp, 2002; Psuty, 1988). On stable and slightly eroding beaches, the dunes tend to grow higher after scarping and recovery of the foredune (Christiansen and Davidson-Arnott, 2004; Psuty, 1988). The aim of this study is twofold: (1) to investigate the relation between longshore transport patterns and longshore grain-size variability and (2) to study the interaction between sediment sorting and dune evolution. For this purpose, a sandy beach with a clear net longshore transport direction—Ängelholm Beach in Sweden—was selected as the study site.

*DOI: 10.2112/JCOASTRES-D-18-00153.1 received 6 November 2018; accepted in revision 24 February 2019; corrected proofs received 3 April 2019; published pre-print online 25 April 2019.*
*Corresponding author: caroline.hallin@tvrl.lth.se


Cross-shore transport processes dominate the sediment sorting in the nearshore (Guillén and Hoekstra, 1996). However, sorting through longshore transport processes can be reflected in longshore variations of the average grain size in the profile (Huisman, de Schipper, and Ruessink, 2016). The median grain size found in the swash zone, at the mid–beach face position halfway between the swash zone and wrack line or berm crest, is commonly used as a reference grain size for the beach profile (Bascom, 1951). At this part of the beach, the temporal variation of grain sizes has been found to be small (Bascom, 1951; Emery, 1960; Narra, Coelho, and Fonseca, 2015). From the reference point, the grain size is typically decreasing in seaward direction, although coarser at the plunge point (Bascom, 1951). Landward of the reference point, the sediment can become either coarser or finer; the finest sediment on the dry beach is typically found in the dunes (Bascom, 1951; Ramsey and Galvin, 1977). The advantages of sampling in the reference point are that it is easily accessible, provides consistent results, and allows for comparisons between different studies (Bascom, 1951).

The reference point is located within the area where sediment is supplied to the beach under accreting conditions and can thereby signify whether the beach is supplied with sediment in the appropriate grain-size range for aeolian transport and dune formation (de Vries *et al.*, 2014; Hoonhout, de Vries, and Cohn, 2015). The range of dune-building grain sizes depends on several site-specific factors (*e.g.*, wind climate, surface moisture, vegetation, and topography) (Bauer *et al.*, 2009; Wiggs, Baird, and Atherton, 2004). The dominant grain

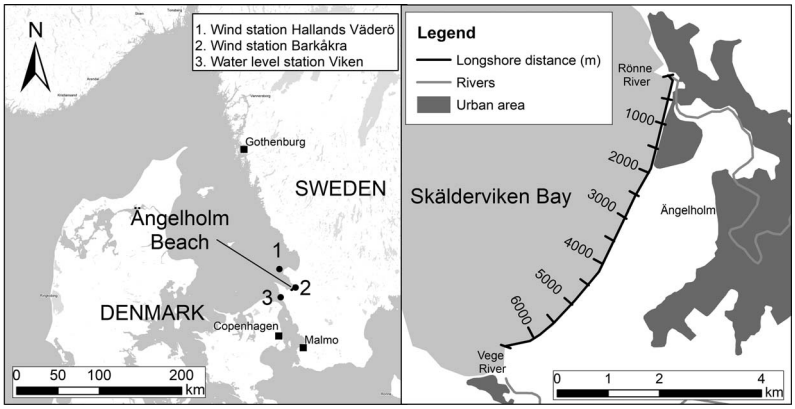


Figure 1. The left panel shows the location of the study area and the Swedish Meteorological and Hydrological Institute (SMHI) measurement stations. The right panel shows Ängelholm Beach, where the longshore distance $x$ is marked along the beach and is referred to throughout the paper.

size in wind-blown sand deposits typically lies between 0.15 and 0.30 mm but may be as fine as 0.08 mm (Bagnold, 1941). However, grain sizes smaller than 0.14 mm are generally not present on sandy beaches because they tend to stay in suspension in the nearshore and be deposited at larger depths (Bagnold, 1963; Ingle, 1966; as cited in Friedman, 1967).

The spatial variation in grain size distributions—both longshore and cross-shore—has in previous studies been used to derive sediment transport patterns (Gao and Collins, 1992; Guillén and Hoekstra, 1996; McLaren and Bowles, 1985). Transport analysis based on grain-size variation has the advantage that it allows long-term processes to be analysed from data representing a snapshot in time (Ramsey and Galvin, 1977). A widely employed grain-size model is the McLaren model (McLaren and Bowles 1985), which relates sediment transport paths to spatial changes in grain-size distribution parameters through statistical analysis. The McLaren model is supposed to be generally applicable to different types of subaqueous sediment transport, such as fluvial transport, delta-lacustrine transport, and longshore transport (McLaren and Bowles, 1985). However, when applied to longshore sediment transport on sandy beaches, the results are mixed—in some cases satisfactory (Mohd-Lokman *et al.*, 1998), whereas in other cases inadequate (Kovaleva *et al.*, 2016; Masselink 1992).

In this study, a set of 58 longshore-distributed sediment samples from Ängelholm Beach are analysed to investigate the relation between grain-size distribution, longshore transport, and dune evolution. Gradients in longshore sediment transport rate are analysed on the basis of observed changes from aerial photos and a nearshore wave propagation model combined with longshore sediment transport calculations. The result is compared with the transport direction indicated when applying the McLaren model. The relation between dune evolution and the longshore variability in grain size is investigated by comparing the reference grain size to the longshore variation in dune height, the rate of change of the vegetation line, and the grain size found in the dunes in previous studies at this beach.

## Ängelholm Beach Study Site

Ängelholm Beach is located in the Skälderviken Bay in southwestern Sweden (Figure 1). The beach is microtidal, and the semidiurnal tide has an average amplitude of about 5 cm and a spring tide amplitude of up to 20 cm (SMHI, 2013). The wind climate is dominated by winds from SW to W (Figure 2). The beach has a sheltered location in the bay but is impacted almost yearly by storm surges and large waves from the NW, causing beach and dune erosion (Palalane *et al.*, 2016). During onshore winds, a significant local wind setup can occur in the bay and the storm surges typically occur in combination with large waves. No wave measurements are available from the area, but the largest simulated wave at the bay mouth had a significant wave height of 5.3 m and a peak period of 9.2 m (Palalane *et al.*, 2016).

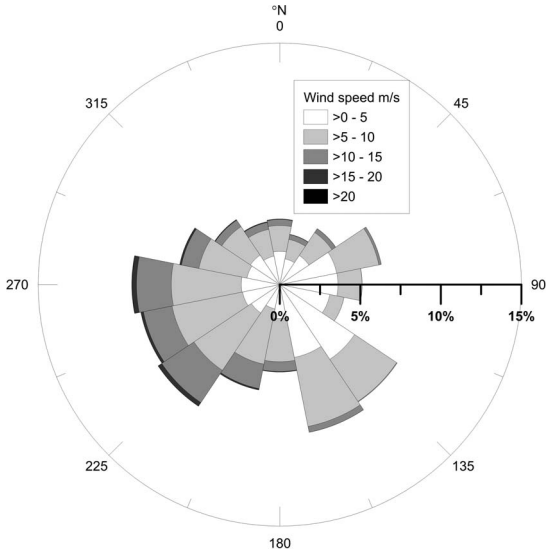


Figure 2. Wind rose compiled with data from 1976 to 2016, which is used for wave hindcasting. The wind climate is dominated by winds from SW to W.

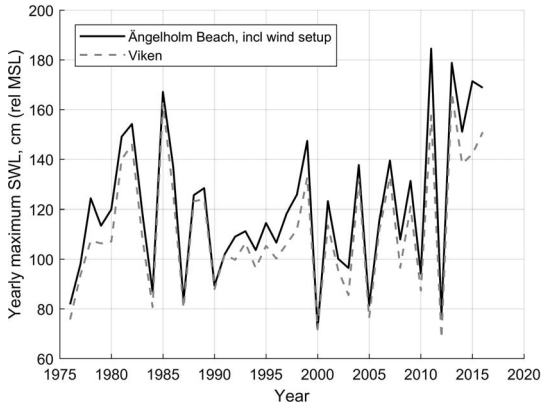


Figure 3. Yearly maximum still water levels (SWL) in 1976–2016 based on measurements from Viken (dashed grey line) and the yearly maximum corrected for local wind setup in Skälderviken Bay (solid black line). The current decade has seen several extreme events compared with the period 1990–2010.

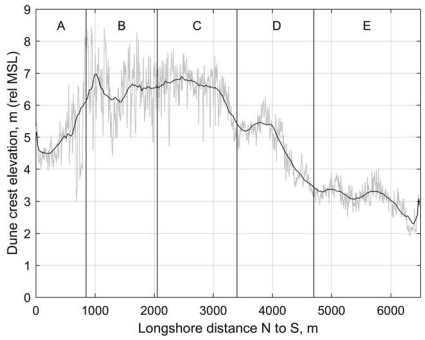


Figure 4. Variation of foredune crest elevation from north to south. The grey line indicates the crest elevation every 2 m alongshore, and the black line is a running average over 400 m. The dunes within the first 850 m are constructed with a gabion core. South of the constructed dunes, the crest elevation increases and is about 6–7 m between $x = 1000$ and 3000 m. Then, the crest elevation decreases in the southward direction down to about 2 m in the south, where no dunes are present.

The yearly maximum still water levels range between 0.8 and 1.8 m above normal (Figure 3). The water levels from station Viken (Figure 1), which is located outside Skälderviken Bay, have been corrected for wind setup according to the method outlined in Palalane *et al*. (2016). Because most storms occur during the winter season, the years in the analysis were defined from July until June the next year. The storms in 2011, 2013, 2014, 2015, and 2016 all caused higher storm surges than observed in the previous two decades.

The beach is situated between two rivers, the Rönne in the north and Vege River in the south, with average flows of 23.5 and 5.0 $m^3/s$, respectively (SMHI, 2009). The amount of sediment supply from the rivers is largely unknown. At a measurement station upstream in the Rönne, where the average flow is about half the flow at the river mouth, the inorganic component of the suspended solids transport has been measured to be $1.8 \times 10^6$ kg/y on average (Brandt, 1996); however, the grain size of the material is unknown. Some erosion has been observed in the river catchments (Karlsson, 2014; Leth, 2014), and specific stretches of the rivers and their tributaries are regularly being dredged to maintain the water depth, which are indications of sediment transport and deposition in the rivers. Even though sandy floodplain deposits are found in some areas near the rivers, the main part of the catchments consists of clay and clayey till. Therefore, most of the sediment transported by the rivers is expected to be finer than the beach sediment and not contribute significantly to the sediment budget of the beach.

Sand deposits are mainly found in shallow water along the coast and a few kilometres inland (Daniel, 1977). The sandy deposits originate from reworked till in the area below the highest Pleistocene coastline, which is about 55–60 m above present mean sea level (MSL). Several kilometres inland from the coast are aeolian deposits that were active until the 19th century when the dunes were stabilized with sand fences and vegetation.

The beach can be divided into five sections by dune shape and crest height (Figure 4); section A: longshore distance $x = 0$–850 m; section B: $x = 850$–2050 m; section C: $x = 2{,}050$–3400 m; section D: $x = 3400$–4700 m; and section E: $x = 4700$–6500 m (Figure 1). Figure 5 shows photos from the different sections together with typical profiles of the dune and dry beach, extracted from the Swedish National Elevation Model from 2010 (Lantmäteriet, 2019).

In the northern part of the beach, section A, the Rönne outlet is fixed with 380-m-long piers. The Rönne has breached the narrow dune row at several occasions, of which 1868, 1902, and 1967 were particularly severe (Almström and Fredriksson, 2011). After the storm in 1967, the dunes were reconstructed with a gabion core. The dune height, defined from the dune foot to the foredune crest, is about 2–4 m. The beach and dunes were nourished with 53,000 $m^3$ of sand taken from the north side of the harbour piers at the Rönne outlet in the year 2000 (Almström and Fredriksson, 2011). Further south in section B, the dunes are higher, 5–6.5 m high, and have been eroding as a result of multiple storms during the last decade. The area behind the dunes is developed, and the dunes function as flood protection for the low-lying hinterland (Palalane *et al*., 2016). After the storms in 2011, 2013, 2014, 2015, and 2016, the dunes were replenished with sediment from the surf zone the following spring. At some of these occasions also the dunes in section A were supplied with sand. In section C, the dune erosion has not been as severe and the dunes have to a larger extent recovered after storm events by aeolian processes (Palalane *et al*., 2016). The dunes here are about 4–5 m high. Further south, in section D, the dune system consists of multiple relict foredune ridges about 2–4 m high. In section E, the dunes are only about 1–1.5 m high, and the beach is wide, low-lying, and moist most of the time.

A previous study at Ängelholm Beach investigated the cross-shore grain-size distribution at three profiles in sections B, C, and D at four occasions (Fredriksson, Larson, and Hanson, 2017). Samples were collected in seven cross-shore distributed sampling points in the subaerial part of the beach, from the

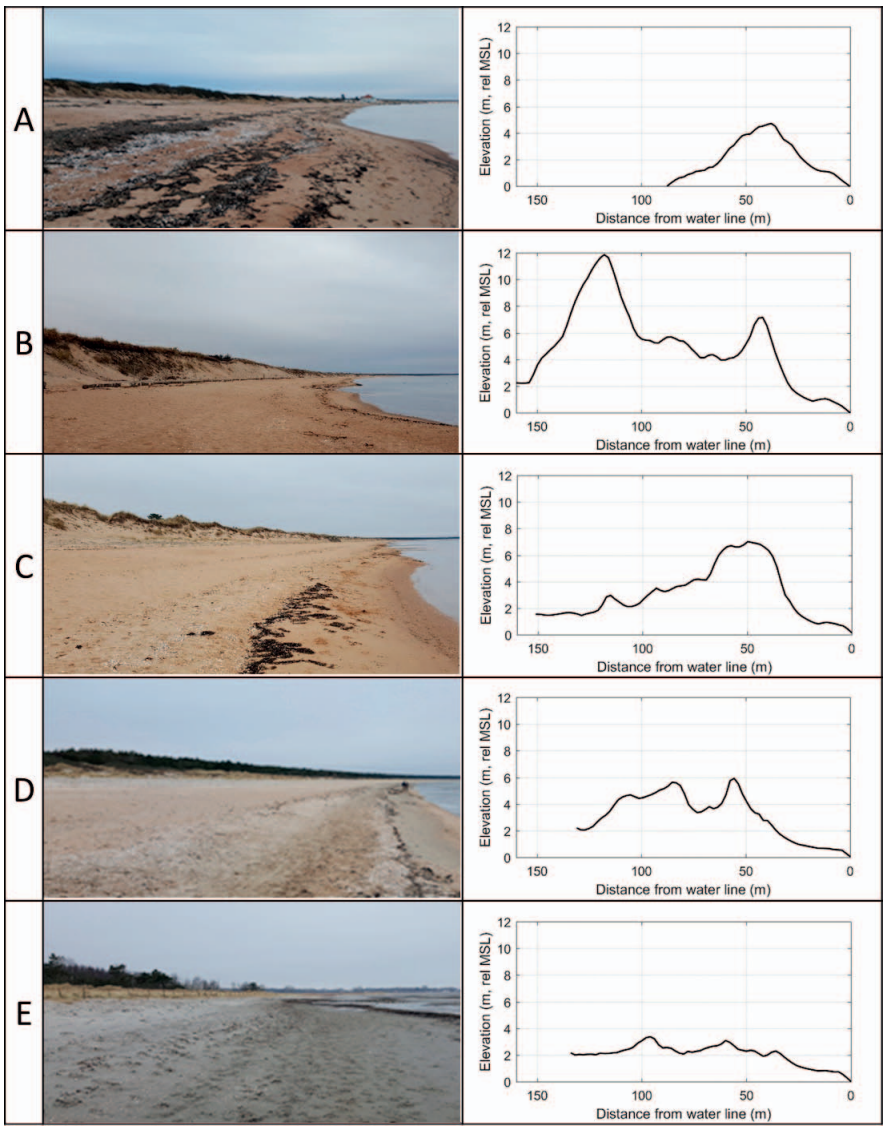


Figure 5. Characteristic subaerial beach and dune profiles in sections A–E. The dune profiles in the right panels are extracted from the national digital elevation model; the distance on the *x* axis is relative to the intersection with MSL. The colour of the beach is changing from more red in the north (section A), where the sand has a larger content of feldspar, toward more white in the south (section E), where quartz is dominant. The photos are taken in the north–south direction.

water line to the dune crest. In all profiles, the median grain size of aeolian-transported sediment found up in the dunes was about 0.2–0.3 mm. In the eroding section B, where the aeolian transport has not been sufficient to recover the storm erosion, the grain sizes found across the beach were in general coarser than the grain size found in the dune. In sections C and D, where dune recovery from aeolian transport was observed, grain sizes in the dune-building fractions were available at all sampling occasions.

The main portion of the bottom sediment in the deeper parts of Skälderviken Bay consists of clay. For this study, the Swedish Geological Survey provided a bathymetric survey from October 2012 (the material cannot be published because of military security restrictions). In this bathymetry, no bars are observed. However, from aerial photos, parallel bars can be detected in section E, and along the entire beach, temporary crescentic subaqueous deposits are visible within 70 m of the shoreline.

## METHODS

Gradients in longshore sediment transport are derived from observations of shoreline change in a series of aerial photos, and from computed sediment transport rates based on simulated wave data. The McLaren model is applied to grain-size data from a set of longshore-distributed samples to test whether the transport patterns are reproduced. The relation between the median grain size and parameters related to longshore transport rate is investigated through correlation

Table 1. *Aerial photos used in the DSAS analysis.*

| Year/Date | Resolution (m) | Spectrum | Collection Agency |
|---|---|---|---|
| Summer 1940 | 1 | B/W | Lantmäteriet[†] |
| Summer 1947 | 1 | B/W | Lantmäteriet |
| Summer 1960 | 0.5 | B/W | Lantmäteriet |
| Summer 2012 | 0.25 | RGB | Lantmäteriet |
| 26 Nov 2014 | 0.05 | RGB | Metria AB/Ängelholm municipality |
| Summer 2016 | 0.25 | RGB | Lantmäteriet |

*B/W = black and white; RGB = red, green, blue colour values*
[†]*Swedish mapping authority.*

analyses. Correlation analysis is also used to explore the relation between dune evolution and sediment sorting and budget. The applied methods are outlined in the following sections.

## Shoreline Change Analysis

The shoreline change analysis was performed with DSAS version 4.4 (Digital Shoreline Analysis System; Thieler *et al.*, 2017), an extension to Esri's ArcGIS with the capability to calculate shoreline change statistics. In this study, shorelines and vegetation lines were digitized from aerial photos (Table 1). To avoid differences in the result related to the coverage from different years, only aerial photos with a complete coverage of the study area were selected (*i.e.* 1940, 1947, 1960, 2012, 2014, and 2016). The aerial photos from the 1940s are an exception, where the photo covering $x = 0$–3250 m is dated to 1947, and the photo covering $x = 3250$–6500 m is dated to 1940.

The vegetation line was based on the most nearshore vegetation that could be identified in the aerial photos. The shoreline was defined as the water line, which was distinct on this microtidal beach. The beach width was computed as the difference between the shoreline and vegetation line for each year.

The rates of change of shorelines and vegetation lines were estimated with the linear regression method LRR. DSAS computes LRR by fitting a least squares regression line to all shoreline points for each shore-perpendicular transect. An alternative computation method is the weighted linear regression WLR, where the estimated error of shoreline position in the observations also is taken into account so that increased weight is given to the more precise observations. In this study, the uncertainty related to seasonal variations, temporary water level changes, resolution, and georeferencing was estimated to 10 m for the aerial photos from the 1940s and 1960s, and 5 m for those from the 2010s. The estimated uncertainties were higher for the older photos because of lower resolution and quality. The LRR method was selected to avoid an unproportionally large effect of recent extreme storms—coinciding with the more precise observations—on the analysis.

The shoreline change was analysed at shore-perpendicular transects with 50-m spacing, and the results were linearly interpolated to the grain size sampling locations.

## Wave Model

Energy-based significant wave height, spectral peak period, and wave direction were calculated at the outer bay using the Sverdrup–Munk–Bretschneider (SMB) formulations for wave hindcasting (USACE, 1984). The formulations were modified with a memory function, as used by Hanson and Larson (2008), so that antecedent wave conditions were taken into account, both for wave growth and decay. The method applied was identical to that described in Palalane *et al.* (2016).

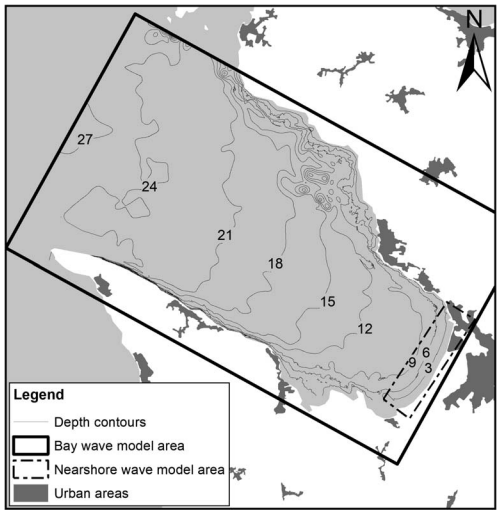


Figure 6. Extent of the bay and nearshore wave model together with the bathymetry of Skälderviken.

A SWAN model (Booij, Ris, and Holthuijsen, 1999) was set up for Skälderviken Bay (Figure 6). The calculated offshore waves were used as input in the SWAN model to simulate the wave climate for the period 1976–2016. A nested modelling approach was used to simulate the nearshore wave propagation, using a 500-m grid size for the bay model and 100 m for the nearshore model (<10 m depth). Because no wave measurements were available for calibration, default model parameter settings were applied.

## Longshore Sediment Transport

The potential longshore sediment transport rates were calculated with the Coastal Engineering Research Center (CERC) formula (USACE, 1984) at 59 positions with 110-m spacing alongshore so that the sampling points were located halfway between the computation points.

Wave heights were extracted every hour from the SWAN model at 5 m depth and transformed to breaking depth using an explicit formula (Larson, Hoan, and Hanson, 2010). The explicit formula computes wave height $H_{sb}$ and wave angle $\alpha_b$ at incipient breaking based on a simplified solution of the wave energy flux conservation equation combined with Snell's law.

The longshore sediment transport rate was calculated using the CERC formula (USACE, 1984):

$$Q_{ls} = \frac{K}{16(s-1)(1-P)} H_{sb}^2 c_{gb} \sin(2\alpha_b) \quad (1)$$

where, $Q_{ls}$ is the potential sediment transport rate integrated across the surf zone, $s$ the relative density of the sediment (typically 2.65), $P$ is the sediment porosity (typically 40%), $c_{gb}$ is the wave group celerity at breaking, and $K$ is an empirical coefficient equal to 0.39. Here, it is assumed that $c_{gb} = (gh_b)^{1/2}$,

where $g$ is the acceleration due to gravity, and $h_b$ is the breaker depth, where $h_b = H_{sb}/0.8$. The orientation of the coastline was taken from the 2-m depth contour, which was slightly smoother than the shoreline and assumed to represent the average coastline orientation of the area where longshore sediment transport occurs.

Sediment transport is defined as positive in the southward direction, $Q_{south}$, and negative in the northward direction, $Q_{north}$. The gross sediment transport rate $Q_{gross}$ is defined as $Q_{net} = Q_{south} + |Q_{north}|$, and the net sediment transport rate $Q_{net}$ as $Q_{net} = Q_{south} + Q_{north}$.

Gradients in net longshore transport rates are computed as the difference in the transport between two consecutive computation points with index $i$, divided by the longshore distance:

$$dQ/dx = \left(Q_{net,i+1} - Q_{net,i}\right)/\Delta x \quad (2)$$

Assuming an equilibrium profile, the potential shoreline change rate, $dy/dt$ (m/y), is computed through:

$$\frac{dy}{dt} = -\frac{dQ}{dx} \times \frac{1}{h} \quad (3)$$

where, $h$ is the height of the active profile from the depth of closure to an upper reference, taken as both the dune foot $h_{df}$ and dune crest position $h_{dc}$ to estimate the shoreline and vegetation line changes. The depth of closure has been estimated to 5 m and the dune foot height to 2 m (Palalane *et al.*, 2016) and are considered constant for all computation points. The dune crest level is varying and was determined from the digital elevation model (Figure 4).

Observed longshore transport gradients are derived from the shoreline and vegetation line changes, $dy_b/dt$ and $dy_d/dt$, through:

$$\frac{dQ_{obs}}{dx} = -\frac{dy_b}{dt} h_{df} - \frac{dy_d}{dt}(h_{dc} - h_{df}) + \frac{V_{nour}}{dt} \quad (4)$$

where, $V_{nour}/dt$ is the nourished volume per meter of beach length divided by the length of the analysis period.

### Sampling and Grain Size Analysis

Samples were collected on 28 March 2018. In total, 58 sand samples were collected at an alongshore spacing of 110 m. The samples were taken from the Bascom reference point located at the mid–beach face position, halfway between the swash zone and wrack line or berm crest (Bascom, 1951).

Samples of 200 g were obtained with a plastic beaker measuring 6 cm in diameter and 4 cm depth. The samples were sieved in a Retsch AS 200 basic shaker for 20 min with half-phi sieve sizes of 2, 1.4, 1, 0.71, 0.5, 0.355, 0.25, 0.18, 0.125, 0.09, and 0.063 mm.

Grain-size statistics were analysed with the computer program GRADISTAT (Blott and Pye, 2001). For the application of the McLaren model, the Folk and Ward (1957) graphical method was used to compute mean $M$, sorting $\sigma$, and skewness Sk, in phi units ($\Phi = -\log_2 d$), where $d$ is the grain size (mm), according to:

$$M = \frac{\Phi_{16} + \Phi_{50} + \Phi_{84}}{3} \quad (5)$$

$$\sigma = \frac{\Phi_{84} - \Phi_{16}}{4} + \frac{\Phi_{95} - \Phi_5}{6.6} \quad (6)$$

$$\mathrm{Sk} = \frac{\Phi_{16} + \Phi_{84} - 2\Phi_{50}}{2(\Phi_{84} - \Phi_{16})} + \frac{\Phi_5 + \Phi_{95} - 2\Phi_{50}}{2(\Phi_{95} - \Phi_5)} \quad (7)$$

where, the subscript of the phi units indicates the percentile of the cumulative distribution.

### McLaren Method

The McLaren model builds on the assumption that lighter grains have a higher probability of being transported than heavier grains and that the deposition of sediment is a selective process that changes the grain size distribution compared with the source sediment (McLaren, 1981).

Transport direction is analysed by comparing all possible pairs of sediment samples in one transport direction with respect to changes in mean grain size, sorting, and skewness. Eight possible combinations of these three parameters exist. Transport in one dominant direction is assumed if a downdrift sample compared with an updrift sample is becoming: (A) finer, better sorted, and more negatively skewed or (B) coarser, better sorted, and more positively skewed. The McLaren model assumes that all possible combinations of changes to statistical distribution parameters have the same probability of occurrence, 1/8, which should be significantly exceeded for cases (A) or (B) above to indicate transport.

For each transport indicator (A and B), a $Z$ test (Equation [8]) is applied to determine whether the number of occurrences $n$ out of the total number of pairs $N$ exceeds the random probability $p$. The null hypothesis $H_0$ is that there is no preferred transport direction: $p \leq 1/8$. The tested hypothesis $H_1$ is that transport is occurring in the analysed direction, $p > 1/8$:

$$Z = \frac{n - Np}{\sqrt{[Np(1-p)]}} \quad (8)$$

The $H_1$ hypothesis is accepted at the 5% significance level if $Z > 1.645$ and at the 1% significance level if $Z > 2.33$.

## RESULTS

The shoreline change analysis and sediment transport rate calculations indicated an almost unidirectional transport from north to south, with erosion in the northern part and accretion in the southern part of the beach (Figures 7 and 11). When the McLaren model was applied to the grain-size data, it predicted significant transport in both directions; however, it was most significant in the wrong direction (Table 2). Among the sediment distribution parameters evaluated in the McLaren model, the mean grain size was the only parameter showing a significant longshore trend (Figure 12). The longshore sediment transport patterns were reflected in the longshore dune evolution, in support of the conceptual model of Psuty (1988) (Figure 14). The details of the results are outlined in the following sections.

### Analysis of Aerial Photos

The rate of shoreline change was calculated based on five aerial photos from 1940 to 2016 by the linear regression method in DSAS (Thieler *et al.*, 2017). The left panel in Figure 7 displays the yearly rate of change for the shoreline and

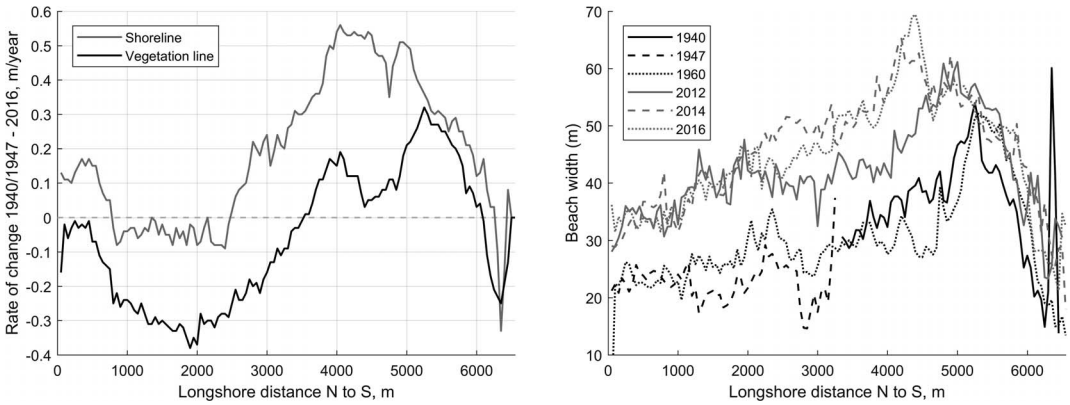


Figure 7. Left panel displays the rate of shoreline (grey line) and vegetation line (black line) change, and the right panel displays the beach width evolution. The shoreline and vegetation line changes follow a similar pattern, but the shoreline is more positive, causing a widening of the beach. The widest part of the beach has moved northward over time.

vegetation line. Positive rates indicate accretion and negative rates erosion. In general, the shoreline shows a more positive rate of change than the vegetation line, both in the eroding and accreting parts of the beach. As a consequence, the beach is becoming wider, which is shown in the right panel of Figure 7. This is probably because of the severe storms during the last decade, which caused large dune erosion that has not fully recovered because of limited aeolian transport. South from $x =$ 5300 m, the rates of change of the shoreline and vegetation line are almost equal; thus, in this part, beach width has been nearly constant over the study period. The widest beach in the observations from 1940 and 1960 was found at $x = 5300$ m. However, in later years, the widest point has progressively moved north and is found in the last observation from 2016 at $x = 4300$ km.

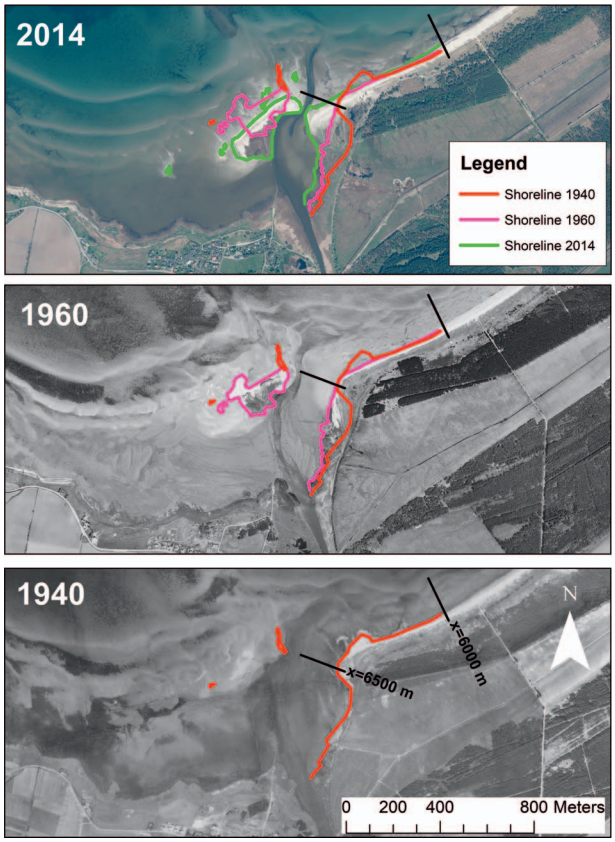


Figure 8. Evolution of the coastline around the Vege River mouth in the southern end of the study area. The red line shows the shoreline in 1940, the magenta line in 1960, and the green line in 2014. The protruding coastline in 1940 has been flattened out, and an island has formed SW of the beach.

The shoreline evolution is positive except at $x = 800$–2500 m and $x = 6300$–6400 m, whereas the vegetation line is only positive at $x = 3500$–6000 m. Thus, the shoreline evolution is explained both by supply from the eroding dunes and gradients in longshore transport. The coastal evolution due only to gradients in longshore sediment transport is probably somewhere between the rate of change of the shoreline and the vegetation line.

At $x = 0$–500 m, the shoreline has advanced, which is explained by a nourishment carried out in 2000. In the southernmost part of the beach at $x = 6200$–6400 m, the beach erosion is probably caused by the interaction between the flow from the Vege River and the longshore current. Figure 8 shows the coastal evolution in the southernmost part of the study area from photos from 1940, 1960, and 2014. In 1940, the river

Table 2. *Result from the McLaren model; n is the number of pairs indicating transport, and Z is the result of the Z test. The total number of pairs in each transport direction is N = 1653.*

| | North to South | | South to North | |
|---|---|---|---|---|
| | *n* | *Z* | *n* | *Z* |
| A: Finer, better sorted, more negatively skewed | 311 | 7.8* | 126 | −6 |
| B: Coarser, better sorted, more positively skewed | 43 | −12.2 | 500 | 21.8* |

**Significant at the 1% level.*

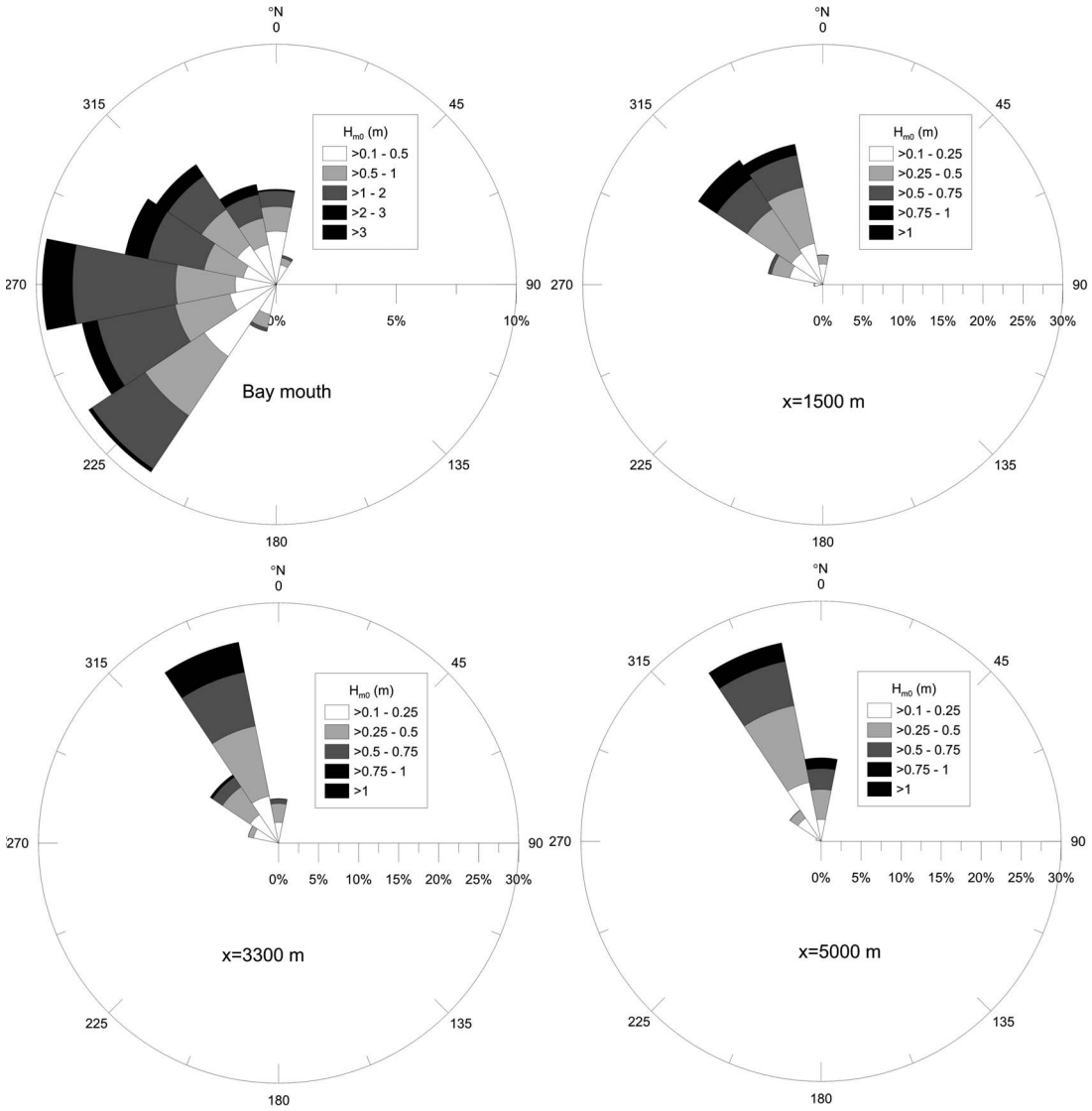


Figure 9. Hindcasted significant wave height during 1976–2016 at the mouth of Skälderviken Bay and at 5 m depth for three locations along the beach. Because of wave sheltering and refraction in the bay, the wave climate is much less energetic and the directional spectrum more narrow. The beach mainly receives waves from NW to NNW.

mouth was at $x = 6500$ m and further north; at $x = 6300$–$6400$ m, the beach was protruding from the coastline. In 1960, this protrusion had been flattened out, and an island had formed on the SW side of the river outlet. In 2014, the island had grown further, and the beach on the updrift side of the river had advanced to the SW.

Altogether, the shoreline change analysis indicates a net sediment transport from north to south and that the northern part of the beach at $x = 0$–$3000$ m is eroding and the southern part at $x = 3000$–$6500$ m is accreting because of gradients in the longshore sediment transport.

## Wave Climate

The wave climate at the entrance of the bay was computed with a modified version of the SMB formula for wave hindcasting and propagated to the nearshore in SWAN. Figure 9 displays wave roses at the outer bay and at three locations in the nearshore zone at 5 m depth: in the northern $x = 1500$ m, central $x = 3300$ m, and southern $x = 5000$ m parts of the beach. The dominant wave direction in the outer bay is W to SW. Along the studied coastline, the waves refract toward the south. The wave climate is more energetic in the northern part of the beach than in the southern part.

The wave climate was simulated for three stationary cases, in which 2-m waves with 5-s periods enter the bay from three different directions: parallel to the bay normal, $\alpha = 0°$, and oblique, $\alpha = \pm 22.5°$ (Figure 10). A positive value means that the waves are entering the bay from a direction south of the bay normal and *vice versa*. The incoming wave direction at the bay

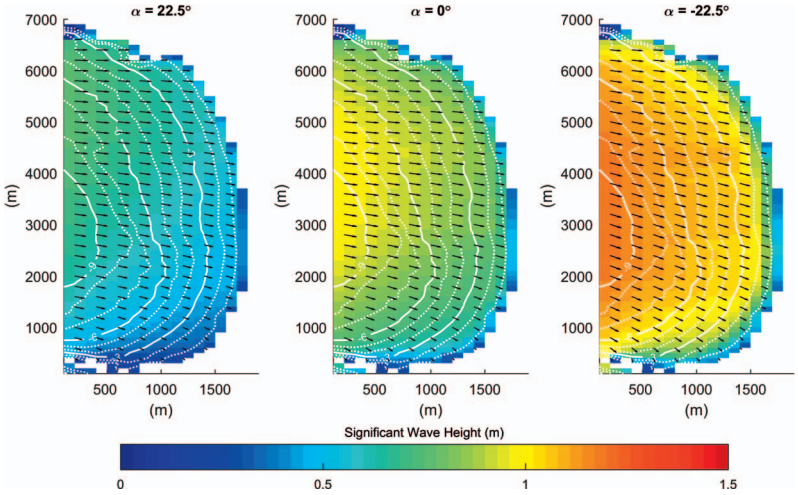


Figure 10. Nearshore wave climate for three stationary SWAN model runs with input of waves with $H_s = 2$ m, $T = 5$ s, and wind speed = 10 m/s in the wave direction from $\alpha = 0°$, –22.5°, and 22.5°, respectively ($H_s$ is significant wave height). The results show that the nearshore wave height is significantly affected by the incoming wave direction, where waves coming from north of the bay normal ($\alpha = -22.5°$) give the largest wave heights because of the geometric shape of Skälderviken Bay. For all cases, the waves refract toward the south before reaching the beach, indicating that the incoming offshore wave direction does not markedly affect the general wave direction in the nearshore.

mouth has a large effect on the wave height nearshore, but only a minor effect on the wave direction, which is quite similar for all three cases. The largest waves relative to incoming waves occur at $\alpha = -22.5°$ because of the bathymetry and geometric shape of the Skälderviken Bay.

## Computed Longshore Transport Rates

The simulated waves at 5 m depth were transformed to breaking depth with the explicit formula, and the longshore sediment transport rate was computed with the CERC formula. The computed potential yearly average transport rates were about 70,000–100,000 $m^3$/y (left panel in Figure 11). At about $x$ = 4000 m, sediment transport decreases because of the presence of a subdued salient. The net transport is almost equal to the gross transport, implying that only a small ratio of the gross sediment is transported against the dominant transport direction from north to south.

The right panel in Figure 11 shows the computed shoreline change based on the potential longshore transport gradients, together with the observed changes of the shoreline and vegetation line. The computed values are about six to seven times larger than the observed, which is not unusual when employing the CERC formula with default values on the empirical coefficient (Smith, Zhang, and Wang, 2003).

The shape of the computed shoreline change deviates from the observations specifically in three parts of the beach. First, at $x = 0$–800 m (section A), the model predicts erosion, whereas accretion is observed, probably because of the nourishment in

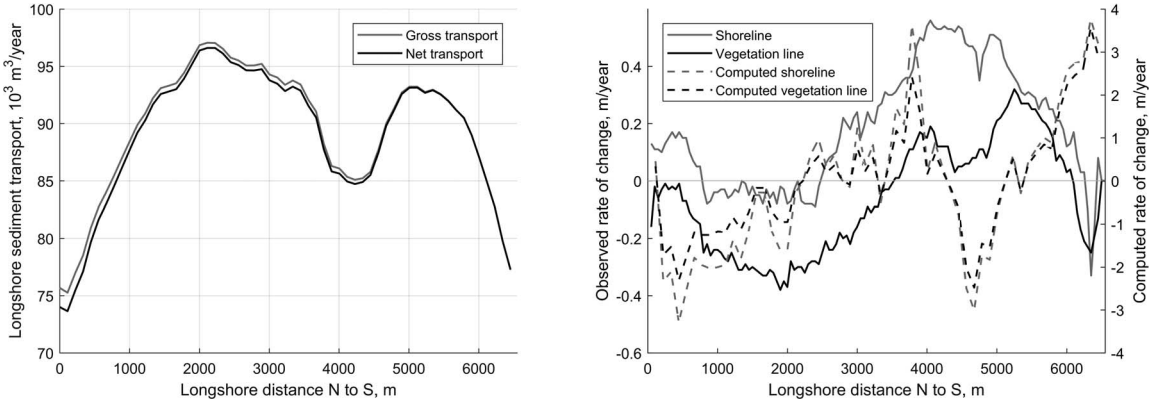


Figure 11. Computed gross and net transport alongshore (left panel) and computed shoreline and vegetation line change compared with observations (right panel). The rate of gross and net transport are nearly the same, meaning that the longshore sediment transport is almost unidirectional from north to south. The gradients in longshore transport are overestimated compared with the observed changes of the shoreline and vegetation line.

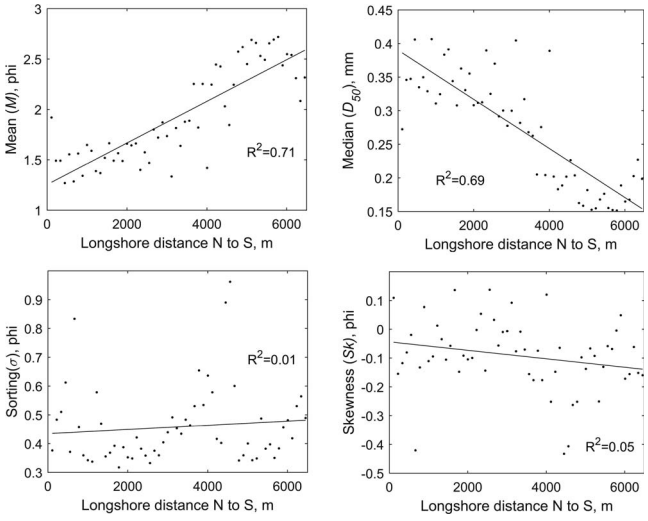


Figure 12. Plot of the mean grain size, sorting, and skewness in phi units according to the Folk and Ward (1957) logarithmic method and the median grain size in millimetres. The mean and median grain sizes have significant longshore trends of becoming finer in the north–south direction. The sorting and skewness show no significant trends alongshore.

this area, which is not included in the shoreline change computations. Second, at $x = 6000$–$6500$ m, the model predicts accretion, whereas erosion is observed. The observed erosion is probably from shoreline changes created by the interaction between the longshore current and the river flow, which is not accounted for in the shoreline change computations. Third, the model predicts erosion at $x = 4300$–$5100$ m, whereas accretion is observed. There is a similar signal in the change of vegetation line; however, the model appears to overpredict

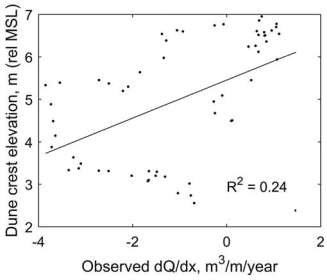


Figure 14. Scatterplot of the dune crest elevation and the observed gradients in longshore sediment transport. In agreement with Psuty's conceptual model, the dunes are lower in the accreting part of the beach and higher where it is eroding or approximately stable.

the influence of the small salient in the coastline at this location, which coincides with the widest point of the beach.

Overall, the computed sediment transport rates indicate that wave refraction in the bay causes an almost unidirectional sediment transport from north to south, in agreement with the observations from the aerial photos.

## Longshore Grain Size Variations

The mean and median grain sizes are becoming significantly finer in the transport direction from north to south (Figure 12). The sediment is also less well sorted and more negatively skewed moving south; however, these trends are not significant (5% level). The results suggest that the mean and median grain sizes are the most relevant parameters to study in relation to longshore sediment transport. However, in engineering applications of today, the median grain size $D_{50}$ in metric units are more commonly used to describe grain size than the phi units (Blott and Pye, 2001); therefore, only $D_{50}$ is further analysed.

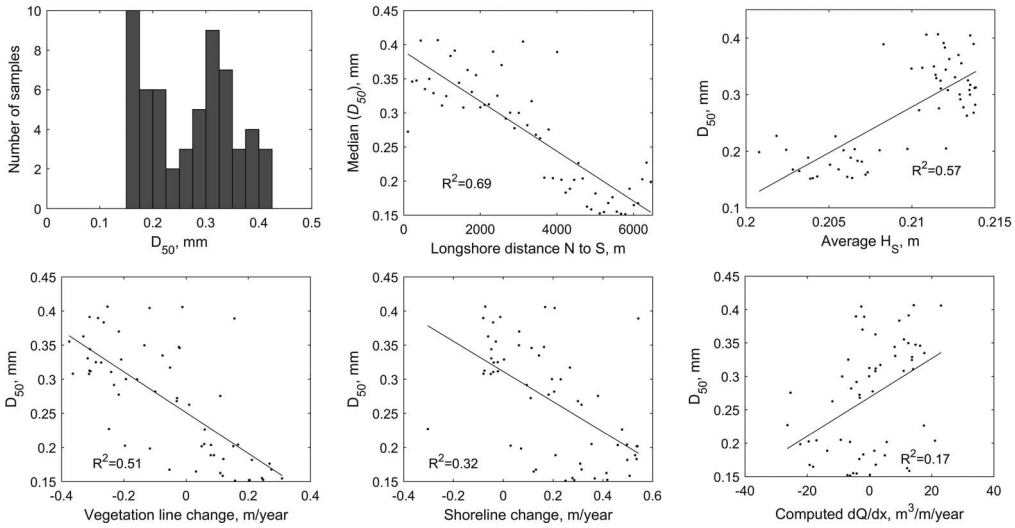


Figure 13. Histogram over median grain size ($D_{50}$) sampled alongshore and linear regression between $D_{50}$ and longshore distance, average significant wave height, observed shoreline change, observed vegetation line change, and computed gradients in longshore transport ($dQ/dx$).

The upper left panel of Figure 13 shows the distribution of $D_{50}$ for all samples. The two peaks in this distribution, one at 0.15 mm and another one at 0.30–0.35 mm, could be explained by wind erosion at the sampling points, because grain sizes ranging from 0.15 to 0.30 mm are most easily entrained and transported by the wind (Bagnold, 1941). In the other panels of Figure 13, $D_{50}$ is plotted against longshore distance, average wave height at the 5-m depth, observed changes of the vegetation line and shoreline, and the computed gradients in longshore sediment transport. The strongest correlation is found with the longshore distance, yielding a coefficient of determination, $R^2 = 0.69$, for a linear fit. There are also marked correlations between $D_{50}$ and the observed changes in the shoreline and vegetation lines; however, linear fits yield a weaker agreement, $R^2 = 0.32$ and $R^2 = 0.51$, respectively. These correlations indicate a relationship between gradients in longshore sediment transport and grain size, as well. However, the result suggests that on this beach, sediment grain size has a stronger correlation to transport direction than the size of transport gradients.

### The McLaren Model

The alongshore variation in grain-size distribution was analysed with the McLaren model to see whether the dominant transport direction could be determined by this method. The result indicates two significant transport directions, from north to south by type A sorting and from south to north by type B sorting (Table 2). The transport from south to north was most significant: 500 out of a total 1653 sample pairs indicate northward-directed transport as the sediment becomes coarser, better sorted, and more positively skewed in this direction, which is opposite to the result of the analysis of aerial photos and the transport computations. On the basis of the analysis of the statistical grain-size distribution parameters in the McLaren model (Figure 12), the mean grain size is found to be the only parameter that can be correlated with longshore sediment transport.

### Dune Morphology

Results in the previous sections have shown that the vegetation line has advanced in the accreting areas of the beach and that the reference grain size there is within the range of dune-building sediment on this beach, about 0.2–0.3 mm (Figures 7 and 13). The dune height was correlated with the observed gradients in longshore transport according to Equation (3) (Figure 14). Although the data exhibit a lot of scatter, there is a weak correlation between sediment budget and dune height. In eroding or more or less stable stretches of the beach, the dunes are high, with crest elevations of about 6–7 m. In the accreting areas where $dQ/dx < -1.5$ m$^3$/m per year, the dunes are lower, with dune heights of about 3–5.5 m.

## DISCUSSION

The analysis of the aerial photos showed that the overall long-term evolution at Ängelholm Beach is erosion in the northern part and accretion in the southern part. The computed sediment transport was almost unidirectional from north to south. When the computed transport gradients were used to compute shoreline change, the rate of change was overpredicted by a factor of six to seven. The empirical coefficient was not calibrated, and the CERC formula has been found to overestimate transport rates in laboratory studies with the same parameter setting (Smith, Zhang, and Wang, 2003). The overestimation of the shoreline change may also be related to the variation of grain size alongshore, which is not accounted for with this simple approach. Furthermore, it is not certain that sand is available within the entire profile along the beach.

Nevertheless, the computed transport direction, the accretion and erosion observed in the aerial photos, and the island developing SW of the beach clearly demonstrate that the dominant longshore transport direction is from north to south. The McLaren model predicted sediment transport in the opposite direction at a 1% significance level, according to transport indicator B—coarser, better sorted, and more positively skewed. This result supports the conclusion by Masselink (1992) that the applicability of the McLaren model to derive longshore transport directions in the nearshore zone is limited.

The unsatisfactory results from the applications of the McLaren model on sandy beaches could be because the assumption of sediment coarsening in the transport direction is not valid in some sandy systems. Studies showing sediment coarsening downdrift (Cipriani and Stone, 2001; McCave, 1978; Schalk, 1938) do all have mixed beach material originating from eroding cliffs, lagoon inlets, or rivers that contain fine sediment that is washed offshore. If large amounts of fine sediment with grains size smaller than 0.14 mm are supplied to a beach (*e.g.*, from rivers or cliff erosion), they may cause coarsening in the downdrift direction as the fine sediment is washed offshore (McCave, 1978; Schalk, 1938). The grain size coarsening is then a result of cross-shore transport processes and should not be considered an indication of longshore transport (McCave, 1978).

Gao and Collins (1992) proposed a modification of the McLaren model based on two-dimensional transport vectors with improvements of the statistical analysis. However, the underlying assumption regarding which combinations of grain-size distribution parameters indicate transport is only slightly modified, and the condition of the coarsening of grain size in the transport direction is still assumed. Thus, for this one-dimensional longshore transport case, the result of their model would be expected to be similar to that of McLaren and Bowles (1985).

The result of the grain size analysis demonstrated that the sediment is becoming finer alongshore in the transport direction. The sediment is coarser in eroding stretches of the beach and finer in accreting stretches. The difference in grain size between the north and south part of the beach is significant, with $D_{50}$ varying from about 0.4 to 0.15 mm, which is expected to affect dune buildup and dune morphology.

There is a large variation in beach and dune morphology alongshore. In the northern part, where the beach is eroding or is more or less stable (sections B and C), the dunes are higher compared with the accreting stretches (sections D and E). The observed dune morphology is in agreement with the conceptual model of Psuty (1988). At eroding or stable beaches, the dunes get scarped, and sediment is translated to the crest or landward side (Davidson-Arnott *et al.*, 2018); on accreting beaches,

incipient foredunes develop in front of the others, creating lower prograding dune ridges (Hesp, 2002). In the most southern part of Ängelholm Beach (section E), the dunes are poorly developed and only about a meter high. In this area, the observed $D_{50}$ was about 0.15 mm, which is smaller than the grain size found in the dunes in previous studies (Fredriksson, Larson, and Hanson, 2017). Such fine grain size leads to reduced aeolian transport by capillary forces keeping the beach wet much of the time.

Fredriksson, Larson, and Hanson (2017) proposed that if sediment in the dune-building range of grain sizes was not available on the beach, there would be no aeolian transport building dunes. In this study, the sediment samples were collected at the Bascom reference point (Bascom, 1951) between the swash zone and berm crest. This part of the beach is built by waves and is an area of deposition on accreting beaches. Thus, if the median grain size in this part of the beach is too coarse or too fine to build dunes at the study site, it is an indication that the supply of dune-building sediment is limited. On the beach, there will be sediment that is both finer and coarser than the median grain size. However, because beach material typically has a fairly uniform distribution (Bascom, 1951), $D_{50}$ can be used to assess whether the bulk of the material on the beach is of the proper grain size to build dunes. The results show that dune-building sediment is available south of $x = 3000$ m (Figure 13), which coincides with the area of accretion and where the vegetation line has advanced (Figure 7). This is also the area where the dunes partly have recovered from storm erosion from aeolian transport (Palalane *et al.*, 2016).

This study is based on sediment sampling at one occasion; thus, temporal grain-size variation cannot be evaluated. The distribution of median grain size within the samples (Figure 13) suggested a possible wind erosion of the sampled material. In future studies, repeated samplings, both longshore and cross-shore, could be used to investigate how the Bascom reference point represents beaches with no astronomical tide. However, because the longshore transport is approximately unidirectional and no nourishments have been carried out since 2000, the conditions are not expected to change significantly at the Bascom reference point (Emery, 1960; Narra, Coelho, and Fonseca, 2015). Huisman, de Schipper, and Ruessink (2016) studied the temporal evolution of grain-size distribution at a mega feeder nourishment, "the Sand Motor," in The Netherlands. When the nourishment was completed, the grain size in the eroding parts coarsened, whereas the grain size in the accumulating parts became successively finer.

The anthropogenic effects on dunes may be significant (*e.g.*, through beach nourishments, sand fences, vegetation wear, and limitations of accommodation space) (Nordstrom, 2000). At the study site, the dunes have partly been created with sand fences, and in section A they are constructed with a gabion core. Vegetation wear from tourists is largest within section B, which might have affected the estimation of the vegetation line and made the dunes more prone to erosion. The nourishment in the year 2000 was accounted for in the transport gradients that were derived from DSAS observations. However, the nourishment is not expected to influence the grain-size distribution in this study, because it has been 18 years since the implementation.

From a coastal management perspective, information on grain-size sorting and the coupling to transport processes is valuable when designing mitigation measures. In the northern part of the beach, the shoreline is retreating, and the dunes, which function as flood protection for the developed hinterland, have during the last decade eroded almost every year without a natural recovery (Palalane *et al.*, 2016). To protect the urban areas and conserve the beach, beach nourishment in sections A and B is a possible mitigation method. To allow for the dunes to recover from aeolian transport, part of the nourished material should be within the range of grain sizes naturally found in the dunes. The longshore sediment transport will continue to deplete the content of fine sediment in the nourished volume, and therefore the nourishment will need to be replenished to maintain the aeolian transport capacity. Typically, materials used for nourishments are selected to be of the same grain size or coarser than the material found on the beach to prevent increased erosion rates. The optimal nourishment scheme to promote aeolian transport should, however, be balanced against feasibility with respect to other transport processes, costs, and requirements for the beach and dune ecology.

## CONCLUSIONS

In this study, the relationship between longshore sediment transport processes and alongshore variations in beach face grain-size distribution parameters was investigated. Analyses of 58 sediment samples along a 6.5-km-long sandy beach, together with shoreline change analyses from aerial photos and longshore sediment transport rate computations, were performed. The results showed that Ängelholm Beach has a nearly unidirectional longshore sediment transport from north to south. The median grain size decreased significantly in the transport direction, from about 0.4 to 0.15 mm. Sediment sorting and skewness did not show any significant longshore trends, which is probably because of sorting through cross-shore transport processes.

The result of the McLaren model indicated significant transport in both northward and southward directions. The northward direction, which is incorrect, was most significant. This result can be explained by the underlying assumption of sediment coarsening in the transport direction being incorrect for sandy beaches. Furthermore, the other transport indicator implying that sediment becomes finer, better sorted, and more negatively skewed was not supported by the sediment analysis in this study; grain size was the only significant indicator of the transport direction.

Sediment sorting by longshore transport processes affects aeolian transport by supplying or depleting the beach with sediment of the appropriate grain size to build dunes. At Ängelholm Beach, the median grain size in the eroding parts of the beach is coarser than the grain size found in the dunes. Sediment sorting by longshore sediment transport explains the limited capacity in the eroding part of the beach to restore storm-eroded dunes. In the most southern part, on the other hand, the sediment is so fine that capillary forces keep the beach wet most of the time and thus decrease aeolian transport. Furthermore, the sediment budget affects dune morphology;

dunes were higher in the eroding or approximately stable parts of the beach and lower in the accreting parts.

The results of this study emphasize the need to incorporate the effect of grain-size sorting in long-term beach and dune evolution models and to consider the importance of sediment supply of the appropriate grain size for dune buildup in coastal management strategies.

## ACKNOWLEDGMENTS

We are grateful to Bas Huisman at Deltares and Marcel Zijlema at TU Delft for advice regarding the SWAN model and relevant literature on grain-size sorting. We are also grateful to Geraldine Thiere at Ängelholm municipality for providing aerial photos and information about their coastal management. Finally, we thank the anonymous reviewers for many useful comments and suggestions to improve our work.

## LITERATURE CITED

Almström, B. and Fredriksson, C., 2011. *Stranderosion i Ängelholms kommun—Inventering av nuvarande förhållande och rekommendationer för framtiden*. Malmö, Sweden: Sweco, 42p (in Swedish).

Bagnold, R.A., 1941. *The Physics of Blown Sand and Desert Dunes*. London: Meuthen, 263p.

Bagnold, R.A., 1963. Mechanics of marine sedimentation. *In:* Hill, M.H.; Goldberg, B.D.; Iselin, C.O., and Munk, W.H. (eds.), *The Sea, Ideas and Observations on Progress in the Study of the Sea*. New York: John Wiley & Sons, pp. 507–528.

Bascom, W.N., 1951. The relationship between sand size and beach-face slope. *Transactions, American Geophysical Union*, 32(6), 866–874.

Bauer, B.O.; Davidson-Arnott, R.G.D.; Hesp, P.; Namikas, S.L.; Ollerhead, J., and Walker, I.J., 2009. Aeolian sediment transport on a beach: Surface moisture, wind fetch, and mean transport. *Geomorphology*, 105(1), 106–116.

Blott, S.J. and Pye, K., 2001. Gradistat: A grain size distribution and statistics package for the analysis of unconcolidated sediments. *Earth Surface Processes and Landforms*, 26(11), 1237–1248.

Booij, N.; Ris, R.C., and Holthuijsen, L.H., 1999. A third-generation wave model for coastal regions: 1. Model description and validation. *Journal of Geophysical Research*, 104(C4), 7649–7666.

Brandt, M., 1996. *Sedimenttransport i svenska vattendrag exempel från 1967–1994*. Norrköping, Sweden: SMHI, *Hydrologi 69*, 20p (in Swedish).

Christiansen, M.B. and Davidson-Arnott, R., 2004. Rates of landward sand transport over the foredune at Skallingen, Denmark and the role of dune ramps. *Geografisk Tidsskrift–Danish Journal of Geography*, 104(1), 31–43.

Cipriani, L.E. and Stone, G.W., 2001. Net longshore sediment transport and textural changes in beach sediments along the southwest Alabama and Mississippi barrier islands, U.S.A. *Journal of Coastal Research*, 17(2), 443–458.

Daniel, E., 1977. *Description to the quaternary map Höganäs NO/Helsingborg NV*. Serie Ae Nr 25. Uppsala, Sweden: Swedish Geological Survey, 92p (in Swedish).

Davidson-Arnott, R.; Hesp, P., Ollerhead, J.; Walker, I.; Bauer, B.; Delgado-Fernandez, I., and Smyth, T., 2018. Sediment budget controls on foredune height: Comparing simulation model results with field data. *Earth Surface Processes and Landforms*, 43(9), 1798–1810.

de Vries, S.; Arens, S.M.; de Schipper, M.A., and Ranasinghe, R., 2014. Aeolian sediment transport on a beach with a varying sediment supply. *Aeolian Research*, 15, 235–244.

Emery, K.O., 1960. *The Sea of Southern California A Modern Habitat of Petroleum*. New York: Wiley, 366p.

Folk, R.L. and Ward, W.C., 1957. Brazos River bar: A study in the significance of grain size parameters. *Journal of Sedimentary Petrology*, 27(1), 3–26.

Fredriksson, C.; Larson, M., and Hanson, H., 2017. Long-term modelling of aeolian transport and beach-dune evolution. *Proceedings of Coastal Dynamics 2017* (Helsingor, Denmark), pp. 715–726.

Friedman, G.M., 1967. Dynamic processes and statistical parameter compared for size frequency distribution of beach river sands. *Journal of Sedimentary Petrology*, 37(2), 327–354.

Gao, S. and Collins, M., 1992. Net sediment transport patterns inferred from grain-size trends, based upon definition of "transport vectors." *Sedimentary Geology*, 81(1–2), 47–60.

Guillén, J. and Hoekstra, P., 1996. The "equilibrium" distribution of grain size fractions and its implications for cross-shore sediment transport: A conceptual model. *Marine Geology*, 135, 15–33.

Hanson, H. and Larson, M., 2008. Implications of extreme waves and water levels in the southern Baltic Sea. *Journal of Hydraulic Research*, 46(2), 292–302.

Hesp, P., 2002. Foredunes and blowouts: Initiation, geomorphology and dynamics. *Geomorphology*, 48(1), 245–268.

Hoonhout, B.A.S.; de Vries, S., and Cohn, N., 2015. The influence of spatially varying supply on coastal aeolian transport: A field experiment. *Proceedings of Coastal Sediments 2015* (San Diego, California), pp. 1–11.

Huisman, B.J.A.; de Schipper, M.A., and Ruessink, B.G., 2016. Sediment sorting at the Sand Motor at storm and annual time scales. *Marine Geology*, 381, 209–226.

Ingle, J.C., 1966. *The Movement of Beach Sand: An Analysis Using Fluorescent Grains*, Volume 5, *Developments in Sedimentology*. Amsterdam, The Netherlands: Elsevier Publishing, Co., 221p.

Karlsson, R., 2014. Phosphorous Levels and Trends in Vege River. Lund, Sweden: Lund University, Master's thesis, 45p (in Swedish).

Kovaleva, O.; Chubarenko, B., and Pupienis, D., 2016. Grain size variability as an indicator of sediment transport alongshore the Curonian spit (South-eastern Baltic Sea). *Baltica* 29(2), 145–155.

Lantmäteriet, 2019. *Product description: GSD-Elevation data, Grid 2+, Document Version: 2.4*, 8p. https://www.lantmateriet.se/globalassets/kartor-och-geografisk-information/hojddata/e_grid2_plus.pdf

Larson, M.; Hoan, L.X., and Hanson, H., 2010. Direct formula to compute wave height and angle at incipient breaking. *Journal of Waterway, Port, Coastal, and Ocean Engineering*, 136(2), 119–122.

Leth, M., 2014. The Role of Vegetation in River Bank Erosion—A Review and Field Study of Two Key Areas in Rönne å. Alnarp, Sweden: Swedish University of Agricultural Sciences, Bachelor's thesis, 35p (in Swedish).

Masselink, G., 1992. Longshore variation of grain size distribution along the coast of the Rhône delta, southern France: A test of the "McLaren model." *Journal of Coastal Research*, 8(2), 286–291.

McCave, I.N., 1978. Grain-size trends and transport along beaches: Example from eastern England. *Marine Geology*, 28(1), 43–51.

McLaren, P., 1981. An interpretation of trends in grain size measures. *Journal of Sedimentary Research*, 51(2), 611–624.

McLaren, P. and Bowles, D., 1985. The effects of sediment transport on grain-size distributions. *Journal of Sedimentary Petrology*, 55(4), 457–470.

Mohd-Lokman, H.; Rosnan, Y.; Ejria, S.; Shazili, N.A.M., and Kassim, K.K.Y., 1998. Deducing sediment transport direction and the relative importance of rivers on a tropical microtidal beach using the "McLaren model." *Environmental Geology*, 34(2/3), 128–134.

Narra, P.; Coelho, C., and Fonseca, J., 2015. Sediment grain size variation along a cross-shore profile—Representative d50. *Journal of Coastal Conservation*, 19(3), 307–320.

Nordstrom, K.F., 2000. *Beaches and Dunes on Developed Coasts*. Cambridge, U.K.: Cambridge University Press, 338p.

Ollerhead, J.; Davidson-Arnott, R.; Walker, I.J., and Mathew, S., 2013. Annual to decadal morphodynamics of the foredune system at Greenwich Dunes, Prince Edward Island, Canada. *Earth Surface Processes and Landforms*, 38(3), 284–298.

Palalane, J.; Fredriksson, C.; Marinho, B.; Larson, M.; Hanson, H., and Coelho, C., 2016. Simulating cross-shore material exchange at decadal scale. Model application. *Coastal Engineering*, 116, 26–41.

Psuty, N.P., 1988. Sediment budget and dune/beach interaction. *In:* Psuty, N.P. (ed.), *Dune/Beach Interaction*. *Journal of Coastal Research*, Special Issue No. 3, pp. 1–4.

Ramsey, M.D. and Galvin, C.J.J., 1977. *Size Analysis of Sand Samples from Southern New Jersey Beaches*. Fort Belvoir, Virginia: Coastal Engineering Research Center, *Miscellaneous Report No. 77-3*, 58p.

Schalk, M., 1938. A textural study of the outer beach of Cape Cod, Massachusetts. *Journal of Sedimentary Petrology*, 8(2), 41–54.

Self, R.P., 1977. Longshore variation in beach sands Nautla Area, Veracruz, Mexico. *Journal of Sedimentary Research*, 47(4), 1437–1443.

Sherman, D.J. and Bauer, O., 1993. Dynamics of beach-dune systems. *Progress in Physical Geography*, 17(4), 413–447.

SMHI (Swedish Meteorological and Hydrological Institute), 2009. *Flödesstatistik för Sveriges vattendrag*. https://www.smhi.se/klimatdata/hydrologi/vattenforing/om-flodesstatistik-for-sveriges-vattendrag-1.8369 (in Swedish).

SMHI, 2013. *Detaljerad översvämningskartering längs Rönne å*. Norrköping, Sweden: SMHI, *Report 2012/2179/9.5* (in Swedish).

Smith, E.; Zhang, J., and Wang, P., 2003. *Evaluation of the Cerc Formula Using Large-Scale Model Data*. Tampa, Florida: University of South Florida, Geology Faculty Publications, *Paper 238*, 13p.

Thieler, E.R.; Himmelstoss, E.A.; Zichichi, J.L., and Ergul, A., 2017. *Digital Shoreline Analysis System (DSAS) version 4.0—An ArcGIS extension for calculating shoreline change (ver. 4.4, July 2017)*. Reston, Virginia: U.S. Geological Survey, *Open-File Report 2008-1278*. doi:10.3133/ofr20081278

Trask, C.B. and Hand, B.M., 1985. Differential transport of fall-equivalent sand grains, Lake Ontario, New York. *Journal of Sedimentary Petrology*, 55(2), 226–234.

USACE (U.S. Army Corps of Engineers), 1984. *Shore Protection Manual (SPM)*. Washington, D.C.: U.S. Government Printing Office, 650p.

Wiggs, G.F.S.; Baird, A.J., and Atherton, R.J., 2004. The dynamic effects of moisture on the entrainment and transport of sand by wind. *Geomorphology*, 59(1), 13–30.